Biased Electrodes for SOL Control in NSTX

S.J. Zweben, R.J. Maqueda*, L. Roquemore, C.E. Bush**, R. Kaita,
R.J. Marsala, Y. Raitses, R.H. Cohen***, D.D. Ryutov***

Princeton Plasma Physics Laboratory, Princeton NJ USA
* Nova Photonics, Princeton NJ USA
**Oak Ridge National Laboratory, Oak Ridge TN USA
***Lawrence Livermore National Laboratory, Livermore, CA USA

Small electrodes were installed near the outer midplane of NSTX to control the width of the scrape-off layer (SOL) by creating a strong local poloidal electric field. Clear increases were seen in the plasma density and potential in between these biased electrodes when the applied E_{pol}xB drift was radially outward. However, little or no change was seen in the D_α emission profile ~1 meter downstream from the electrodes along the magnetic field, implying that the poloidal electric field did not propagate this far along B.

DRAFT – 5/7/08

1. Motivation and Previous Experiments

The present experiment was motivated by the theory that the scrape-off layer (SOL) width in a tokamak could be increased by non-axisymmetric electrical biasing of divertor plates [1-3]. Such biasing would create a local poloidal electric field and radial E_{pol}xB drift larger than the normal radial flow velocity, thereby moving the local SOL strike region radially. It was also suggested that the flows created by this biasing could increase the SOL turbulence and therefore broaden the SOL width. This theory was developed for divertor plate biasing, but similar ideas were proposed for RF-sheath generated convective cells near the outer midplane [4].

These ideas have been tested in several previous experiments. In JFT-2M [5] an electrical bias of +120 volts was applied to an inner wall divertor plate and a poloidal electric field of ~1 kV/m was measured at the midplane where the magnetic field lines connected to the biased plate. In MAST [6] an electrical bias of +80-120 volts was applied to 6 divertor 'ribs', and a clear movement of the D_α emission in the expected ExB drift direction was seen at these ribs. In CASTOR [7] an electrode was biased +100-200 volts in the SOL, and a poloidal electric field of up to 5 kV/m was created on flux surfaces connected to the electrode and a strong poloidal modulation of the radial particle flux was measured. In related experiments, a positive DC plate bias in DITE changed the floating potential in a probe ~2.5 mm away along B [8], a positive DC and 30 kHz bias in TEXT were detected ~12 m away along B [9], and a 60 KHz probe bias in W7-AS was observed at a distance up to ~12 m away along B [10]. Thus several previous biasing experiments have created local poloidal electric fields in the SOL, which is encouraging for the development of control techniques.

2. NSTX Electrode and probe hardware

The electrode configuration used for this experiment is shown in Fig. 1. Four 3 cm x 3 cm stainless steel electrodes were mounted in a boron nitride holder with a gap of ~1 cm between them. Each electrode could be independently biased up to ±100 volts with respect to the local vessel wall and draw up to 30 amps per electrode for positive bias, and 10 amps per electrode for negative bias. The electrode power supplies were modulated at 50 Hz to allow comparison of electrode on and off states, and the voltages and currents were digitized at 20 kHz.

This electrode holder was mounted ~20º below the outer midplane and oriented so that the electrodes were spaced along the local poloidal direction and the total magnetic field was normal to the plane of the electrodes. The innermost radial edge of the electrode holder was ~1 cm behind the leading edge of an RF antenna limiter located just behind the electrode holder. Thus the electrodes were in contact with the SOL plasma in only one direction along B. The field lines in this direction extended a distance of from ~1 to ~8 meters along B before hitting any other object in the SOL, depending on the details of the plasma equilibrium.

The effect of the biasing was measured locally with a set of flush-mounted stainless steel Langmuir probes installed in the electrode holder, as shown in Fig. 1. The probes were 3 mm in diameter and probe voltages and currents (for 5 probes) were digitized at 200 kHz. The effect of the biasing was also measured ~1 meter downstream along the B field by the gas puff imaging (GPI) diagnostic. Further information concerning the design and construction of the electrodes and probes are described elsewhere [11].

3. Plasma conditions and biasing waveforms

The experiments described here were made using a standard NSTX deuterium plasma configuration with a current of I=0.8 MA, a toroidal field of B=4.5 kG, neutral beam heating power of P=2-4 MW, and a lower-single-null diverted geometry with a discharge duration of ~0.5 sec (#127046-054). These discharges had both H-mode and L-mode periods during biasing (the biasing itself did not affect this transition). The plasma density at the electrodes varied with the 'outer gap', i.e. the distance between the last closed flux surface and the outer midplane RF antenna limiter, which varied over the discharge from ~10 cm to 5 cm for these experiments. Since these electrodes and probes were at least ~1 cm behind the RF limiter, all of these measurements described in this paper were made in the "far SOL" [12]. Thus it is not surprising that this electrode biasing never caused perceptible changes in the global plasma parameters in these experiments, e.g. in the stored energy or impurity radiation .

An example of electrode voltages and currents waveforms for one of these discharges is shown in Fig. 2. For this and all other cases described in this paper, electrodes E2 was biased at -90 volts, electrode E3 was biased at +90 volts, electrode E4 was biased at -90 volts, and electrode #1 was floating (the 3 biased electrodes were modulated in phase at 50 Hz). The ExB drift direction between electrodes #2 and #3 was in the outward radial direction. The biased electrode currents in the L-mode period were typically ~4 amps in the positive electrode and ~0.5 amps in the negative electrode during L-mode, and half that during H-mode. The (I,V) characteristic of these electrodes was nearly flat above about ±50 volts, with a ratio of electron/ion saturation current of ~8.

Also shown in Fig. 2 is the signal from probe P3b (between electrodes #2 and #3), which was biased steadily at +45 volts for this case (i.e. near electron saturation current). This probe current signal (which is approximately proportional to the local plasma density) increased significantly when the electrodes were biased, both during H-mode and L-mode. The electron temperature inferred from probe sweeps in probe P3a during a similar shot showed $T_e \sim 10\pm5$ eV , and the approximate (lower limit) to the plasma density inferred from the electron current using $I_e = ½nev_eA$ was $n \sim 10^{11}$ cm^{-3}. The same qualitative behavior shown in Fig. 2 was seen in each of four other similar discharges during this same series, and in several other plasma conditions including Ohmic and RF heated discharges.

4. Effects of biasing on radial profiles near the electrodes

The effect of this biasing on the radial profiles between electrodes #2 and #3 was measured by the four probes P3a-P3d. For all these cases the bias was -90 volts on E2 and +90 volts on E3, with the E_{pol}xB the drift radially outward direction between the electrodes. Fig. 3(a) shows the radial profiles of the electron current measured when the probes were biased at +45 volts, i.e. near electron saturation (#127054). Each point represents the average over several ~10 msec periods of either bias "on" or "off" during this discharge. The x-axis is the radial probe position with respect to the center of the electrodes. It is clear that the electrode biasing causes an increase in all of these probe currents, e.g. by a factor of x3-5 for L-mode (0.3-0.4 sec) and x3-10 for H-mode (0.2-0.27 sec) .

Fig. 3(b) shows the effect of this biasing on the floating potential profile when these probes were floating (#127052). The electrode bias caused a small (≤5

volt) increase in the floating potential for the two probes nearest the electrodes (P3a,P3b), but not for the probes farther out radially (P3c,P3d). Note that this small change in the floating potential had a negligible effect on the probe currents since the probes were operating near electron saturation.

No significant changes in either the electron current or the floating potential were seen in probe P2 between electrode #2 (-90 volts) and electrode #1 (floating). In general, a single negatively biased electrode had little or no effect on the local density or floating potential seen by probes on either side of it, while a single positively biased electrode caused an increase in the floating potential of both adjacent probes by about 5-20% of the positive electrode bias voltage.

The electron temperature also was measured with these probes during a similar discharge in which the probe bias was continuously swept ±45 volts in 0.5 msec time intervals (#127053). The resulting temperatures in probe P3a were estimated to be T_e~10±5 eV [11], but given these uncertainties it was not clear whether the biasing changed the local electron temperature. Therefore the large changes seen in the electron saturation current during biasing were very likely due to electron density changes and not electron temperature changes.

5. Effects of biasing on turbulence near the electrodes

Part of the motivation for this experiment was to see if a poloidal electric field changed the local plasma turbulence, since this could broaden the SOL. Previous experiments have shown an effect of biasing on SOL turbulence [13], but

those experiments were mainly intended to create a radial electric field and not a local poloidal electric field.

Fig. 4 shows the effects of biasing on various aspects of the turbulence as measured by the radial probe array between electrodes #2 and #3 for the same discharge as Fig. 3 (#127054). These data points are again the averages over several ~10 msec periods of either bias "on" or "off" during this discharge, and are separated into L- and H-mode periods. The x-axis is again the radial probe position with respect to the center of the electrodes.

Fig. 4(a) shows that the relative fluctuation levels (i.e. rms/mean) in the electron saturation current decrease from ~100% without biasing to ~50% with biasing for both L- and H-mode periods; however, the floating potential fluctuation levels increase slightly with biasing (not shown). Fig. 4(b) shows that the autocorrelation times for the electron saturation current signals (i.e. time for the autocorrelation function to reach 0.5) are about the same with or without biasing for the L-mode case, and Fig. 4(c) shows that the correlation coefficient between the innermost probe and the other probes was about the same with or without biasing for the L-mode case. For the H-mode case, the autocorrelation times and correlation lengths were significantly higher with biasing, apparently due to small ELMs which reached the probes only when the electrodes were biased. These autocorrelation times and radial correlation lengths in the absence of ELMs are similar to those measured previously using GPI in NSTX [14].

6. Effects of Biasing on D_α Light Emission

The effect of electrode biasing was also evaluated using the GPI diagnostic ~1 meter downstream along B from the electrodes. The GPI diagnostic measures the D_α light emission from a nearby deuterium gas puff. Figure 5 shows images and radial profiles from this diagnostic for the L-mode period for the same shot used for Figs. 3 and 4 (#127054), averaged over ~10 msec either during bias "on" (red) or bias "off" (black). The location and radial scale of this D_α scan was the approximately the same as for the probe array results in Figs. 3 and 4, i.e. between electrodes #2 and #3, as mapped along field lines to the GPI location. The alignment between the probes and the GPI images was made by identifying regions of high correlation between the turbulence seen in the probes and in the GPI images, and this alignment agreed well with EFIT modeling of the field lines [11].

The result of Fig. 5 was that there was little or no systematic difference between the D_α profiles with or without biasing, either near the peak of D_α emission or near the radial location of the electrodes. Since the GPI light is proportional to the local density, this implies that the large density profile changes seen near the electrodes in Fig. 3 did not propagate to the GPI diagnostic ~1 meter away along B. There were some subtle changes in the motion of the turbulence in the GPI images correlated with electrode biasing, but a description of these is beyond the scope of this paper. Thus it seems that the high frequency density fluctuations were correlated ~1 meter along B whereas the low frequency changes due to biasing were not.

7. Discussion

This paper described the effects of biased electrodes intended to create a local poloidal electric field in the far-SOL of NSTX. The radial profiles of the plasma density, floating potential, and turbulence were measured by probes located between the biased electrodes (Figs. 2-4). Measurements were also made of the radial profile of D_α light ~1 meter downstream along the magnetic field (Fig. 5).

The main result of this experiment was an increase in the plasma density between the electrodes by a factor of x3-10 during ±90 volt biasing, as shown in Fig. 4(a). This result is at least qualitatively consistent with the theory that the SOL density will increase when the local plasma is driven outward by the E_{pol}xB drift created by biasing [1-3]. Thus a local control of the SOL plasma density has been obtained in this experiment.

Another result was that the floating potential increased by only ~5 volts next to the electrodes and did not change at all ~2 cm from the electrodes, as shown in Fig. 3(b). Thus the voltages in the plasma are less than those at the electrodes and have a short range across the magnetic field. Similar results have been seen in previous experiments on SOL biasing [8-10]. It was also seen (but not shown here) that a single positively biased electrode affects the local potential much more than a single negatively biased electrode. These results are at least qualitatively consistent with the theory of the sheath effects on the plasma potential [2,3].

Electrode biasing did not qualitatively change the local plasma turbulence, as shown in Fig. 4. However, the autocorrelation time and radial correlation length increased during biasing in H-mode, as shown in Figs. 4(b) and 4(c), apparently

due to small ELMs reaching the probes during biasing. This effect might eventually be useful to help broaden the SOL width in discharges with ELMs.

A clear result from these experiments was that the electrode biased at +90 volts drew ~5-10 times more current than the electrode biased at -90 volts, as illustrated in Fig. 2. Although this (electron/ion) current ratio was lower than the nearby probes (~10-20), it was much higher than expected ratio of ~1 for a "double probe" model [2] in which the distant wall along B acts as the other electrode. This implies that there was a significant cross-B-field electron current to the positive biased electrodes in this experiment, the origin of which is unknown.

In order to quantitatively compare the observed effects of this biasing with theory, we will need to understand how far the applied electric field penetrated along and across B. The applied field of ~180 volts/cm would have created a v_{rad} ~$5x10^6$ cm/sec, i.e. ~50 times more than the normal radial flow speed in this region. However, the effects on the SOL density depend crucially on the parallel and perpendicular size and magnitude of the electric field in the plasma itself. This electric field penetration physics most likely involves the complicated mechanisms of cross-field mobility (e.g. viscosity, neutrals, turbulence), such as discussed in the context of probe theory [15]. For example, the large cross-field currents inferred for positive biasing could 'short out' the poloidal electric downstream along B, which could explain the small effect of biasing on the D_α profiles seem by GPI (Fig. 5).

In summary, the plasma density in the far-SOL of NSTX was successfully controlled by a local poloidal electric field created using biased electrodes. It remains to be seen whether this technique can also be applied to control the SOL

width at the divertor plate strike point of a tokamak as originally proposed [1-3]. This control has so far required a positive electrode bias and a relatively large electrode power (~0.4 MW/m^2), so it will be important to improve the efficiency of this scheme for practical applications. However, the present configuration might still be useful to control the SOL around relatively small structures such as RF antennas or helium pumping ducts in future tokamaks.

Acknowledgments: We thank Jose Boedo, R. Maingi, and V. Soukhanovskii for help with the design and execution of these experiments. *This work supported by U.S. DOE Contract # DE-AC02-76CH03073.*

Figure Captions:

Fig. 1: Electrode and Langmuir probe configuration in this experiment. The four electrodes are 3x3 cm and flush-mounted into this boron nitride holding structure located just below the outer midplane of NSTX. The electrodes are separated in the poloidal direction and the local magnetic field was normal to their surfaces. The 3 mm diameter probes are flush-mounted adjacent to each electrode and also arrayed in the radial direction between electrode #2 and #3.

Fig. 2: Waveforms of typical electrode voltages and currents vs. time for the discharges described in this paper (B=4.5 kG, I=0.8 MA). Electrodes #2 and #3 were biased at -90 volts and +90 volts and drew currents of ~0.5 Amps and ~4 Amps (respectively). All electrode voltages were modulated at 50 Hz. At the bottom is the current from probe #P3b which was biased steadily at +45 volts in this discharge. The probe current increased each time the electrodes were biased, both before and after the H-L transition at 0.275 sec. For clarity, all of these waveforms were smoothed to reduce the large turbulent fluctuations.

Fig. 3: Effects of electrode bias on the radial profiles of probe current and floating potential as measured by probes P3a-P3d (#127054). The x-axis is the radial probe position with respect to the center of the electrodes. The probe currents in Fig. 3(a) increased by x3-10 during biasing at all radii for both L-mode and H-mode. During biasing the floating potentials in Fig. 3(b) increased by ~4-5 volts in the probe nearest the electrodes (P3a), but not in the probes farther outward (#127052).

Fig. 4: Effect of electrode bias on radial profiles of turbulence as measured by probes P3a-P3d (#127054). The relative fluctuation level in Fig. 4(a) goes down with biasing, but is still large even with biasing (~0.5). The autocorrelation times in Fig. 4(b) and the radial correlation lengths in Fig. 4(c) were nearly independent of biasing, except for the H-mode case with biasing, which are affected by small ELMs. The x-axis is the radial probe position with respect to the center of the electrodes.

Fig. 5: Effect of bias on D_α light emission radial profile measured by the GPI diagnostic ~1 meter downstream along B between electrodes #2 and #3. These images and profiles were each averaged over ~10 msec, and the horizontal axis is the same as for Figs. 2 and 3. Red images and profiles are when the electrodes were "on", and black were for electrodes "off". There was little or no systematic difference in these profiles with or without biasing in these experiments.

References

[1] R.H. Cohen, D.D. Ryutov, Nucl. Fusion 37, 621 (1997)

[2] D.D. Ryutov et al, Plasma Phys. Cont. Fusion 43, 1399 (2001)

[3] R.H. Cohen, D.D. Ryutov et al, Plasmas Phys. Cont. Fusion 49, 1 (2007)

[4] D. A. D'Ippolito, J.R. Myra et al, Phys. Fluids B **5**, 3603 (1993); J.R. Myra and D.A. D'Ippolito, Phys. Plasmas 3, 699 (1996)

[5] J. Hara, Y, Uesugi et al, J. Nucl. Mat. 241-243, 338 (1997)

[6] G. Counsell et al, J. Nucl. Mat. 313-316, 804 (2003); G. Counsell et al, 30th EPS Conference, Vol. 27A, P-3.202 (2003)

[7] J. Stockel, P. Devynck et al, Plasma Phys. Cont. Fusion 47, 635 (2005)

[8] R.A. Pitts and P.C. Stangeby, Plasma Phys. Cont. Fusion 32, 1237 (1990)

[9] D.L. Winslow et al, Phys. Plasmas 5, 752 (1998)

[10] H. Thomsen, M. Endler et al, Plasma Phys. Cont. Fusion 47, 1401 (2005)

[11] L. Roquemore et al, to be submitted to RSI (2008)

[12] J.-W. Ahn, J.A. Boedo, et al submitted to Phys. Plasmas (2008)

[13] G. van Oost et al, Plasma Phys. Cont. Fusion 54, 621 (2003)

[14] S.J. Zweben et al, Phys. Plasmas 13, 156114 (2006)

[15] V.A. Rozhanski et al, Nucl. Fusion 39, 613 (1999); A. Carlson, Phys. Plasmas 8, 4732 (2001)

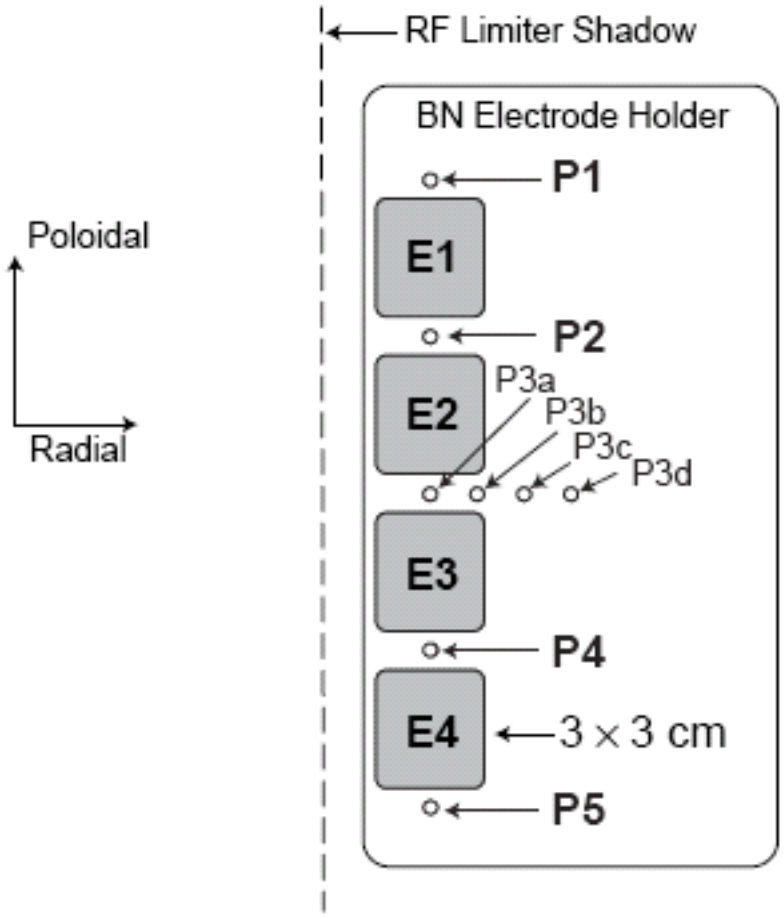
RF Limiter Shadow
BN Electrode Holder
P1
E1
P2
E2
P3a
P3b
P3c
P3d
E3
P4
E4
3 × 3 cm
P5
Poloidal
Radial

Fig. 1

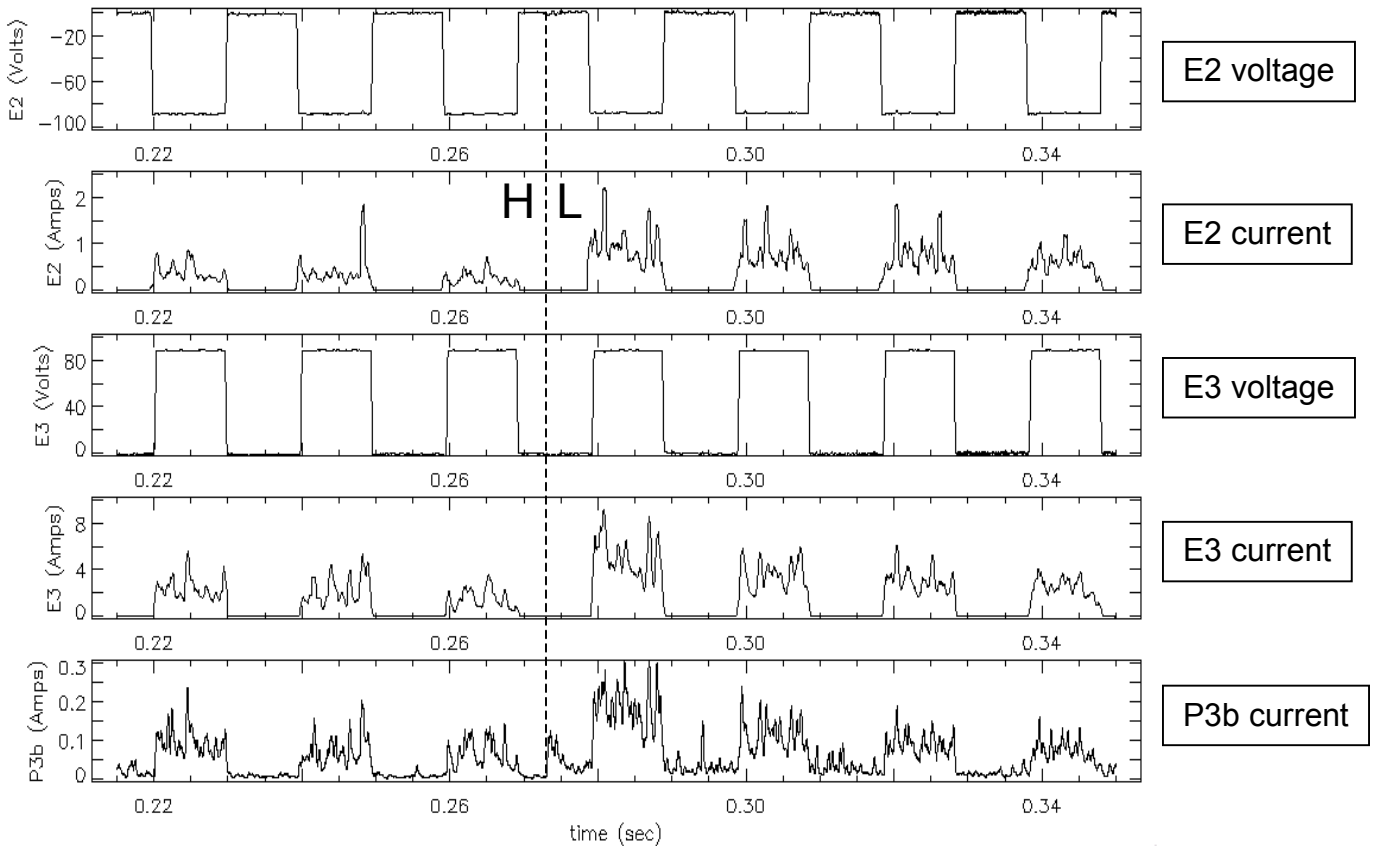
E2 (Volts)
−20
−60
−100
0.22
0.26
0.30
0.34
H
L
E2 (Amps)
2
1
0
E3 (Volts)
80
40
0
E3 (Amps)
8
4
0
P3b (Amps)
0.3
0.2
0.1
0
time (sec)
E2 voltage
E2 current
E3 voltage
E3 current
P3b current

Fig. 2

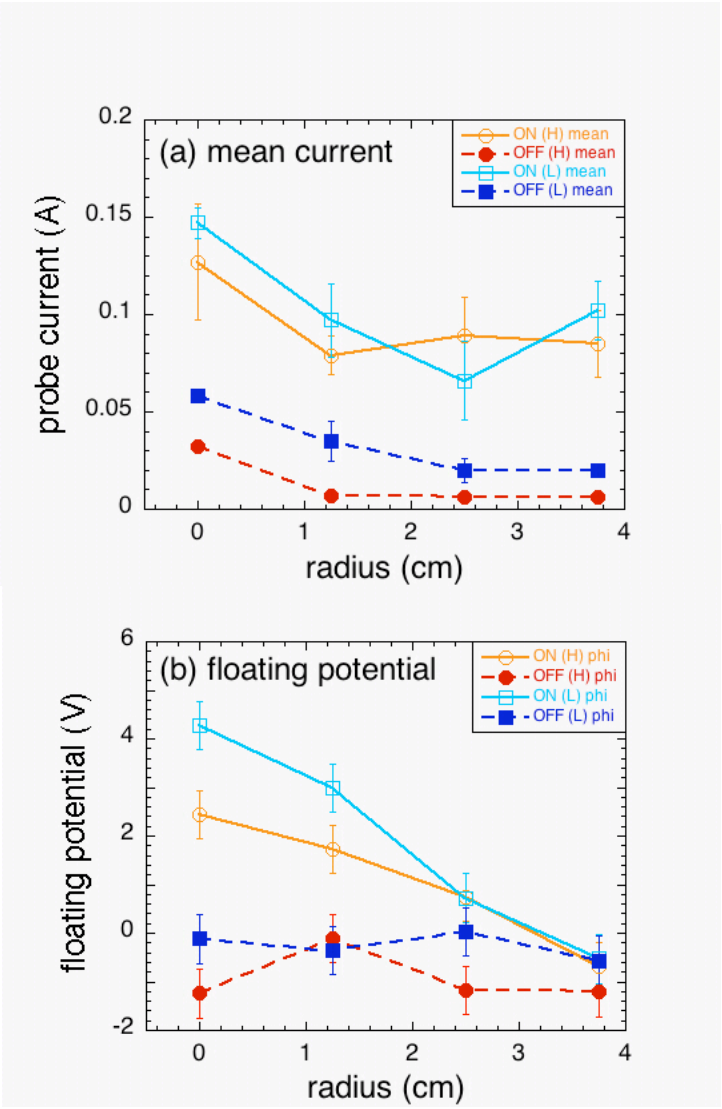
(a) mean current
ON (H) mean
OFF (H) mean
ON (L) mean
OFF (L) mean
probe current (A)
0.2
0.15
0.1
0.05
0
0
1
2
3
4
radius (cm)
(b) floating potential
ON (H) phi
OFF (H) phi
ON (L) phi
OFF (L) phi
floating potential (V)
6
4
2
0
-2
0
1
2
3
4
radius (cm)

Fig. 3

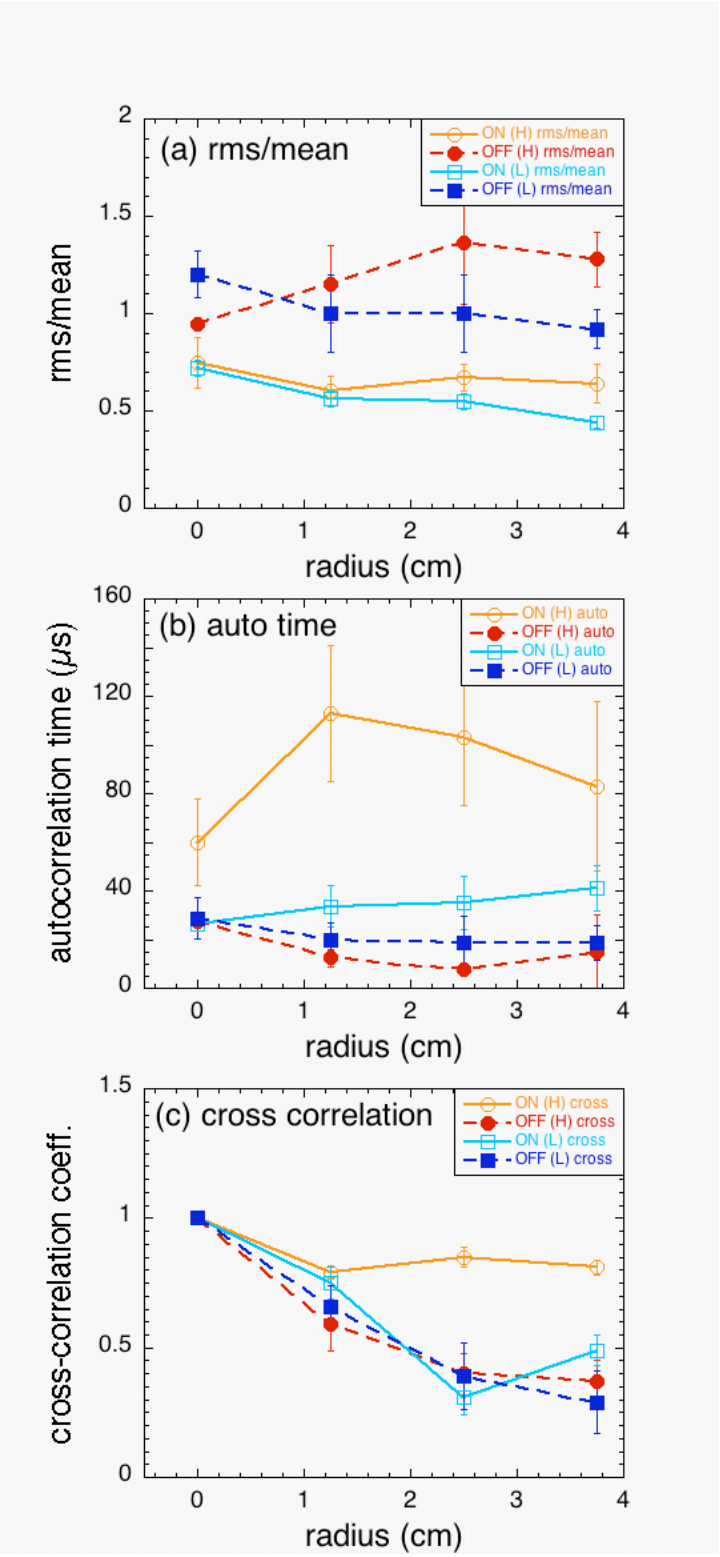
(a) rms/mean
ON (H) rms/mean
OFF (H) rms/mean
ON (L) rms/mean
OFF (L) rms/mean
rms/mean
radius (cm)
(b) auto time
ON (H) auto
OFF (H) auto
ON (L) auto
OFF (L) auto
autocorrelation time (μs)
radius (cm)
(c) cross correlation
ON (H) cross
OFF (H) cross
ON (L) cross
OFF (L) cross
cross-correlation coeff.
radius (cm)

Fig. 4

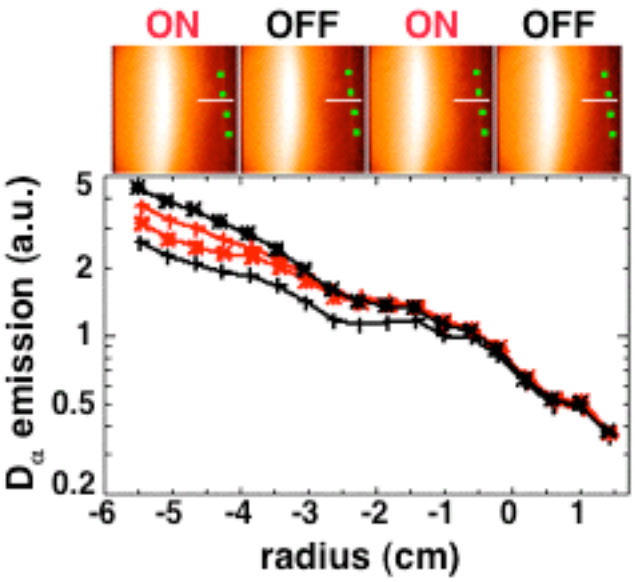

Fig. 5